Indian Journal of Chemistry
Vol. 61, June 2022, pp. 659-670

A comparative theoretical study of three isomeric benzotriazolylpropanamides

Meryem Evecen*

Department of Physics, Faculty of Arts and Sciences, Amasya University, Amasya-05100, Turkey

*E-mail: meryem.evecen@amasya.edu.tr

Received 8 April 2021; accepted (revised) 21 December 2021

Structural, vibrational and molecular electrostatic potential of the isomeric benzotriazolylpropanamides (2-methyl-3-(1H-benzotriazol-1-yl)propanamide, 2-methyl-3-(2H-benzotriazol-2-yl)propanamide and N,N-dimethyl-3-(1H-benzotriazol-1-yl)propanamide) molecules in the ground state have been investigated using different theoretical methods with same basis set. The spectral results obtained from the quantum chemical calculations are in a good agreement with the experimental results. Thermodynamic properties (heat capacity, entropy and enthalpy) at different temperatures are also calculated and discussed by using same methods. Besides, electronic and nonlinear optical properties were investigated in detail. Nonlinear optical property calculations of the molecules indicate that the materials can be used as nonlinear optic materials.

Keywords: Benzotriazolyl, DFT, NLO, MEP

Benzimidazole and its derivatives have been studied for decades[1] and drugs having this heterocycle moiety as main element have been widely used in clinic.[2,3] Benzotriazoles are considered as a promising class of bioactive heterocyclic molecules and exhibit a range of biological activities as antimicrobial, antiprotozoal, antimycotic, anthelmintic, antimycobacterial, antioxidant, antiemetic antitumor, antiviral agent, anti-inflammatory, potassium channel activator, some inhibitors, etc.[4-8] Therefore, benzotriazole appears a very interesting scaffold in the drug discovery and development processes. Besides di- and tridentate pyrazolyl-based ligands play an important role in the design of supramolecular assemblies of metal complexes.[9] As shown in this paper, quantum chemical methods are useful for investigating three benzotriale derivatives, with pyrazolyl-based ligand 3-(pyrazol-1-yl)propanamide.

Due to significance of these molecules and their derivatives, we have investigated these molecules (Fig. 1, 2), using the density functional theory in more detail. The chemical formulae of these molecules are given as:

(1) 3-(1H-benzotriazol-1-yl)-2-methylpropanamide ($C_{10}H_{12}N_4O$)
(2) 3-(2H-benzotriazol-2-yl)-2-methylpropanamide ($C_{10}H_{12}N_4O$)
(3) 3-(1H-benzotriazol-1-yl)-N,N-dimethylpropanamide ($C_{11}H_{12}N_4O$).

We performed theoretical calculations for structural characteristics, vibrational spectroscopic analysis, molecular electrostatic potential (MEP), frontier molecular orbital analysis, NLO, UV and thermodynamic properties of the title molecules.

Computational Methods

Gaussian 09 software package has been used to perform geometry optimizations and total energy calculations by DFT (B3LYP, HF) method with the 6-311++G(d,p) basis set.[10] Visualization of the structure and the analysis of the outputs have been carried out with Gauss-View software.[11] The harmonic vibrational frequencies were calculated at the same level of theory for the optimized structure and the obtained frequencies were scaled by 0.961 (B3LYP) and 0.892 (HF). The TD-DFT technique

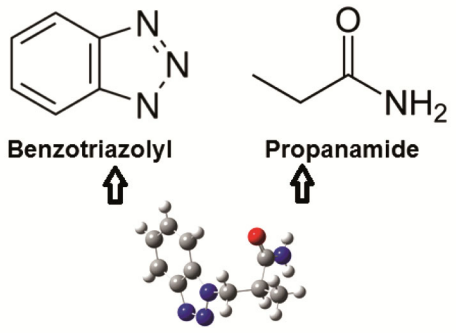

Fig. 1 — Initial molecular geometry of molecule (1)

was employed for acquiring theoretical UV-visible spectra of all molecules in the both gases and ethanol solvent.

Results and Discussion

Structural properties

First, the initial molecular geometry of molecule (1) was directly taken from the X-ray diffraction experimental results without any constraints.[9] Next, from the optimized geometry of molecule (1), the initial geometries of molecules (2) and (3) were obtained using Gauss-View software program. Finally, we made geometry optimizations for molecules (1), (2) and (3) using B3LYP and HF. By considering Fig. 3 and Table 1, the calculated values for the single C–N bond lengths of all molecules were found as 1.40 Å at the B3LYP and HF methods. These values are also consistent with the experimental results (Table 1).[9] Similarly, the C=O separations are in a narrow range around 1.23 Å and are therefore virtually equal with those observed in related functionalized propanamides.[12-15, 9] A comparison of the experimental and calculated bond lengths (without H) are seen in figures for the molecule (Fig. 3).

As seen from Table 1, most of the optimized theoretical bond lengths of the molecules agree with each other while experimental bond lengths are slightly shorter. Similar results were also observed in

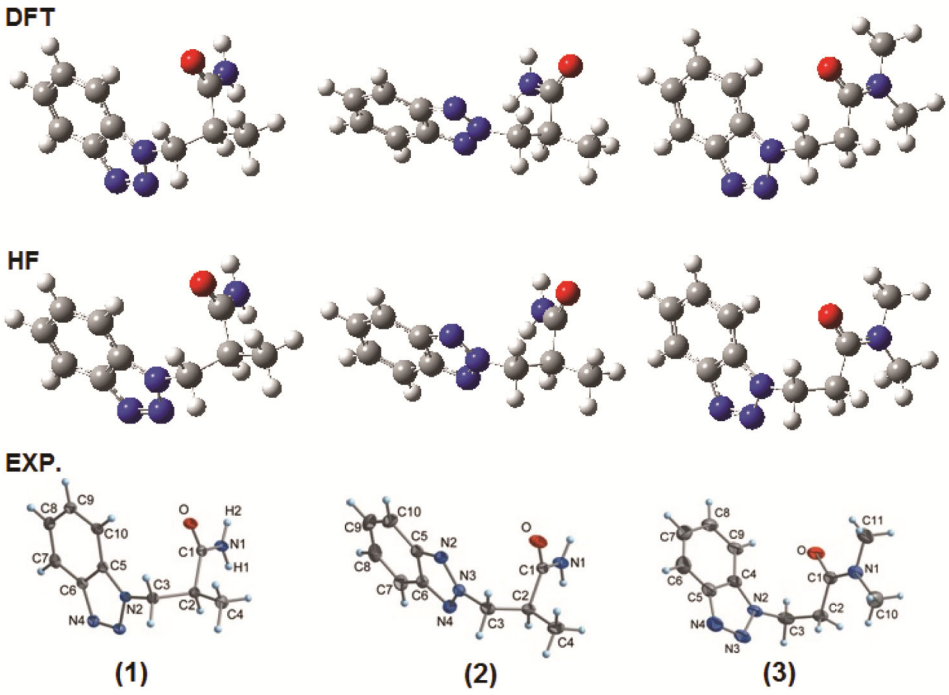

Fig. 2 — Theoretical geometric structure with B3LYP, HF and Ortep-3 diagram[9] of molecules (1,2,3)

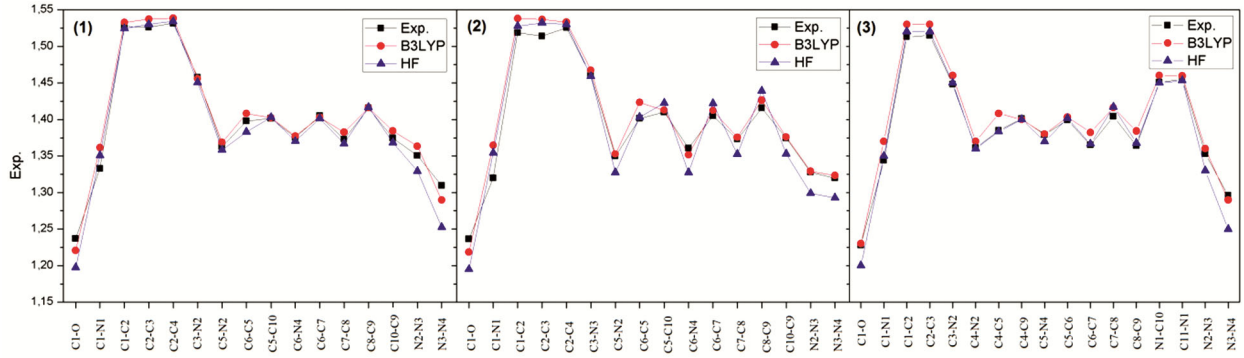

Fig. 3 — Correlation between theoretical and experimental bond lengths of molecules (1), (2) and (3)

Table 1 — Selected bond lengths of molecules (1), (2) and (3)

1(2)	1		2		3	3	
Parameters	Exp.	B3LYP/HF	Exp.	B3LYP/HF	Parameters	Exp.	B3LYP/HF
Bond lengths (Å)					*Bond lengths (Å)*		
C1=O	1.2369 (13)	1.22/1.20	1.2364 (16)	1.22/1.19	C1=O	1.228 (2)	1.23/1.20
C1—N1	1.3329 (14)	1.36/1.35	1.3199 (18)	1.36/1.35	C1—N1	1.344 (2)	1.37/1.35
C1—C2	1.5271 (14)	1.53/1.52	1.5187 (18)	1.54/1.53	C1—C2	1.513 (2)	1.53/1.52
C2—C3	1.5261 (14)	1.54/1.53	1.514 (2)	1.54/1.53	C2—C3	1.515 (2)	1.53/1.52
C2—C4	1.5316 (14)	1.54/1.53	1.5255 (18)	1.53/1.53	N1—C10	1.451 (2)	1.46/1.45
C3—N2(N3)	1.4576 (13)	1.46/1.45	1.4598 (17)	1.47/1.46	C3—N2	1.448 (2)	1.46/1.45
C5—N2	1.3628 (13)	1.37/1.36	1.3498 (18)	1.35/1.33	C4—N2	1.361 (2)	1.37/1.36
C5—C10	1.4014 (14)	1.40/1.40	1.410 (2)	1.41/1.42	C4—C9	1.401 (2)	1.40/1.40
C6—N4	1.3752 (13)	1.38/1.37	1.3607 (18)	1.35/1.33	C5—N4	1.379 (2)	1.38/1.37
N2—N3	1.3505 (12)	1.36/1.33	1.3276 (16)	1.33/1.30	N2—N3	1.3535 (19)	1.36/1.33
N3—N4	1.3096 (13)	1.29/1.25	1.3198 (16)	1.32/1.29	N3—N4	1.296 (2)	1.29/1.25

Table 2 — Selected bond angles and dihedral angles of molecules (1), (2) and (3)

1(2)	1		2		3	3	
Parameters	Exp.	B3LYP/HF	Exp.	B3LYP/HF	Parameters	Exp.	B3LYP/HF
Bond angles (º)					*Bond angles (º)*		
O-C1-N1	123.48 (9)	122.55/122.51	123.67 (12)	122.90/122.67	O-C1-N1	121.60 (14)	122.16/122.61
O-C1-C2	120.43 (9)	115.87/121.28	119.91 (12)	122.10/121.65	O-C1-C2	120.14 (15)	120.10/119.78
N1-C1-C2	116.03 (9)	115.87/116.18	116.40 (11)	114.99/115.67	N1-C1-C2	118.25 (14)	117.73/117.57
C3-C2-C1	110.96 (8)	110.02/110.05	110.76 (11)	110.15/109.81	C3-C2-C1	112.71 (13)	112.41/112.55
N2(N3)-C3-C2	112.50 (8)	113.51/113.15	112.65 (11)	113.39/112.82	N2-C3-C2	113.14 (14)	113.06/112.86
N4-C6-C5	108.40 (9)	108.54/107.97	108.31 (12)	108.19/107.65	N4-C5-C4	108.56 (16)	108.58/107.99
N2-C5-C6	104.07 (9)	103.62/103.56	108.57 (12)	108.13/107.68	N2-C4-C5	104.46 (14)	103.60/103.56
N2-C5-C10	133.36 (9)	130.66/134.34	129.88 (13)	130.80/131.22	N2-C4-C9	133.38 (16)	134.30/134.43
N3(N2)-N2(N3)-C3	119.41 (8)	119.46/119.54	121.07 (11)	121.72/121.64	N3-N2-C3	119.52 (13)	118.99/119.13
N4-N3-N2	108.81 (8)	109.60/110.69	102.93 (11)	117.40/116.90	N4-N3-N2	109.52 (13)	109.65/110.75
Torsion angles (º)					*Torsion angles(º)*		
O-C1-C2-C3	47.10 (12)	50.90/50.36	45.53 (16)	82.10/76.29	O-C1-C2-C3	-16.2 (2)	17.21/17.07
N1-C1-C2-C3	−135.56 (9)	-131.10/-131.80	-136.47 (12)	-98.63/-104.52	N1-C1-C2-C3	164.77 (15)	-164.17/-164.97
C1-C2-C3-N2(N3)	70.99 (10)	68.47/66.76	59.74 (14)	64.72/64.30	C1-C2-C3-N2	-72.24 (18)	79.85/76.07
C10(C5)-C5(N2)-N2(N3)-C3	-0.74 (18)	0.79/2.41	179.62 (14)	176.41/177.91	C9-C4-N2-C3	1.8 (3)	-177.89/3.82
C2-C3-N2(N3)-N3(N2)	82.84 (11)	82.14/77.90	65.73 (15)	43.57/53.59	C2-C3-N2-N3	-78.81 (17)	80.61/76.43

both bond angles and dihedral angles (Table 2). The torsion angle C1-C2-C3-N (DFT/HF) between the amide group and the 1H-benzotriazol-1-yl residue is 68.47/66.76º (molecule 1) and 79.85/76.07º (molecule 3), respectively, which is consistent with the literature.[9,15] By contrast, the same torsion angle in the 2H-benzotriazole-derived molecule 2 is considerably smaller at 64.72/64.30º. It can be seen from Table 2 that the calculated bond and torsion angles are in agreement with each other and other experimental values. For all strctural parameters, results obtained using B3LYP functional are in better agreeement with expermental results than results calculated with HF. The observed differences in bond parameters can be explained by the fact that the intra and intermolecular interactions with the neighboring molecules are absent in gas phase, whereas the experimental results correspond to interacting molecules in the crystal lattice.

In order to compare the theoretical results with the experimental values, root mean square error (RMSE) is used. RMSE is computed using theoretical methods and those obtained from X-ray diffraction.[9] In Fig. 3, calculated RMSE for B3LYP and HF bond lengths are 0.012 Å and 0.019 Å for molecule (1), 0.016 Å and 0.023 Å for molecule (2) and 0.013 Å and 0.015 Å for molecule (3), respectively. Similiarly bond angles (see Fig. 4) are 1,273° and 0.794° for molecule (1), 1,825° and 0.819° for molecule (2) and 0,438° and 0.693° for molecule (3), respectively. As far as

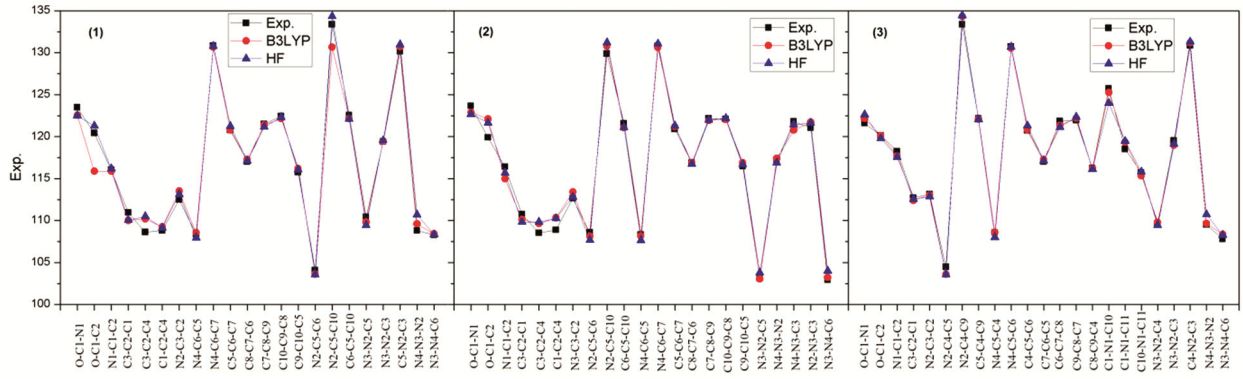

Fig. 4 — Correlation between theoretical and experimental bond angles of molecules (1), (2) and (3)

Table 3 — Comparison of the experimental and calculated vibrational frequencies (cm^{-1}) of molecules (1), (2) and (3)

Assignments [a] (1,2)	Exp. (1,2)	B3LYP*/HF**(1)	B3LYP*/HF**(2)	Assignments [a] (3)	Exp. (3)	B3LYP*/HF**(3)
ν (NH_2) as	3307	3571/3529	3546/3516	ν (C−H) s Alifatic	3082	3073/2996
ν (NH_2) s	3208	3444/3407	3423/3399	ν (C−H) as Alifatic	3050	3059/2965
ν (C−H) s	3155	3079/3006	3075/2999	ν (C−H_2) s	3015	2961/2887
ν (C−H) as	2968	3074/2997	3070/2994	ν (C−H_3) s	2967	2941/2864
ν (C−H_3) s	2930	3078/2857	3075/2909	ν (C−H_3) s	2939	2898/2821
ν (C=O) s	1685	1683/1714	1693/1770	ν (C−H_3) s +	2911	2891/2815
α (N−H)	1442	1558/1582	1561/1585	ν (C=O) s	1644	1638/1672
α (C−H_2)	1315	1421/1355	1430/1383	ν (C−N) α (C−H_2)	1452	1423/1482
ν (C−N)	1226	1211/1143	1237/1234	ω (C−H_2)	1414	1417/1332
τ (CCO)	780	751/722	748/731	ν (C−N)	1338	1313/1251
τ (NCC)+ ω (C−H)	742	724/665	731/663	ν (N=N)	1298	1294/1194
				ω (C−H_3)	1151	1121/1045
				ν (C=C)	942	982/966
				β (CCC)	761	765/753
				τ (NCC)+ ω (C−H)	743	737/666

[a] ν, stretching; α, scissoring; ω, wagging; τ, torsion; s, symmetric; as, asymmetric; *, 0.961 and **, 0.892 by scaled

RMSE calculations are concerned, B3LYP functional gives accurate bond length and angle values for all compunds except for the bond angles of molecule (1).

Spectral Properties

Vibrational spectra

The final optimized structures (Fig. 2) are then confirmed to have all real vibrational states at the same theory level (no negative vibrational frequency). Molecules (1) and (2) contain an equal number of atoms, 27, and have 75 normal modes of vibrations, respectively. But the molecule (3) including 28 atoms has 78 normal modes of vibrations. Selected experimental[9] and computed IR vibrational frequencies and their values for molecules (1), (2) and (3) are presented in Table 3. The IR spectra contain some characteristic stretching vibrations of the C-H, CH_2, C=O, C=C, C-C, C-N and NH_2 groups.

The infrared spectra of the compounds (1) and (2) show characteristic bands of amide group. Here, the observed NH_2 asymmetric and NH_2 symmetric stretching mode of molecule (1) are 3571(3529) and 3444(3407) cm^{-1} for B3LYP(HF), similarly it is 3546(3516) and 3423(3399) cm^{-1} for molecule (2). These values are compatible with the values of 3389 cm^{-1} and 3192 cm^{-1} in Wang's study.[16] As more consistent with the results, it was found as 3422 and 3329 cm^{-1} for B3LYP/6311++G(d,p) by Asli.[17] The hetero aromatics holding an N–H group absorption peak in the region 3500 – 3220 cm^{-1} are ascertained to N–H stretching and the position of absorption within this general region is connected with the scale of hydrogen bonding.[18] Donna et al. found the crystal structures of 1 and 2 comprise infinite arrays formed by N—H…O and N—H…N bridges.[9] The infrared bands at 1722 cm^{-1} were attributed to the asymmetric stretching vibrations of C=O bands.[19] It was observed

that there is a strong C = O asymmetrical stretching band formed near 1700 cm^{-1} (Table 3). Other values given in Table 3 can be interpreted by considering vibrational peaks seen in Fig. 5. Consequently, the calculated vibrational frequencies are in good consistency with both results. According to the results for similar molecules, our results are in good agreement with the literatüre.[12-16]

UV-visible absorption studies

The UV–visible absorption spectrum is utilized to analyze the charge transfer phenomena in organic molecules. Electronic spectra of molecules (1-3) have been studied using UV-visible spectroscopy and TD-DFT calculations for each method (DFT, HF). The comparison between the UV-visible spectra is shown in Fig. 6. The spectrum of the (1-3) in both gases and solvent has two strong bands for DFT (~200 and ~250 nm) and HF (~170 and ~220 nm). It is seen that the wavelength (λ_{max}) is slightly shifted because of solvent effects. The frontier molecular orbitals involved in the transitions for these bands are given in Table 4 which includes the comparative values of the absorption spectra for the two methods. Various electronic absorption assets such as the maximum absorption wavelength (λ), the oscillator strength (f), the excitation energy (E) and the assignments of electronic transitions in both gaseous and ethanol solution are enumerated in Table 4. The electron transition among ground and excited states makes a small contribution to hyperpolarizability. The simulated UV-visible absorbance spectrum of the molecular structure is portrayed in Fig. 6. It reveals that for all of the molecules, there are two simulated maximum absorption wavelengths. We also listed both gas and solvent (ethanol) phase for different methods in Table 4.

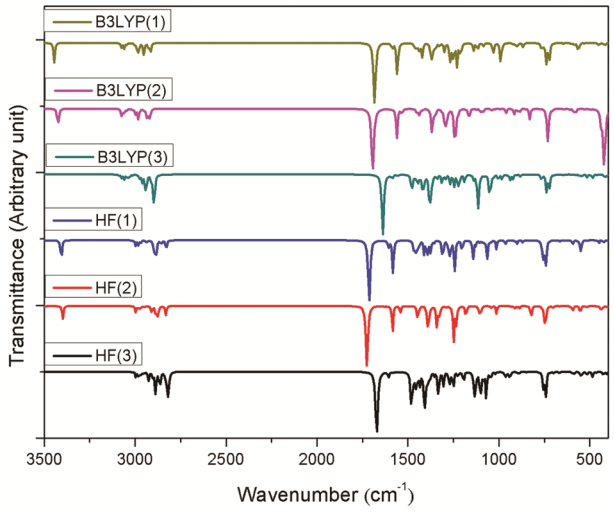

Fig. 5 — Comparison of the B3LYP and HF vibrational frequencies (cm^{-1}) for molecules (1), (2) and (3)

FMO analysis

The FMOs play an important role in the electric and optical properties as well as in chemical reactions and UV-Vis spectra.[20] The graphical representation of FMOs of all molecules are illustrated in Fig. 7. The energy gap between the highest occupied molecular orbital (HOMO) and the lowest unoccupied molecular orbital (LUMO) is very important in determining the chemical activity of the molecule. The HOMO particularly donates electrons, whereas LUMO accepts them.[20]

Energy gaps of molecules (1) and (3) are larger than that of molecule (2). An electronic system with a larger energy difference between HOMO–LUMO orbital (E_{gap}) should be less reactive than one having a smaller gap. Because, getting electrons from a low level HOMO and adding electrons to a high level LUMO is not energetically favorable. The value of the energy barriers between the HOMO and LUMO of the molecule (1) are 5.16 and 9.70 eV for the B3LYP and HF methods, respectively. From Fig. 7,

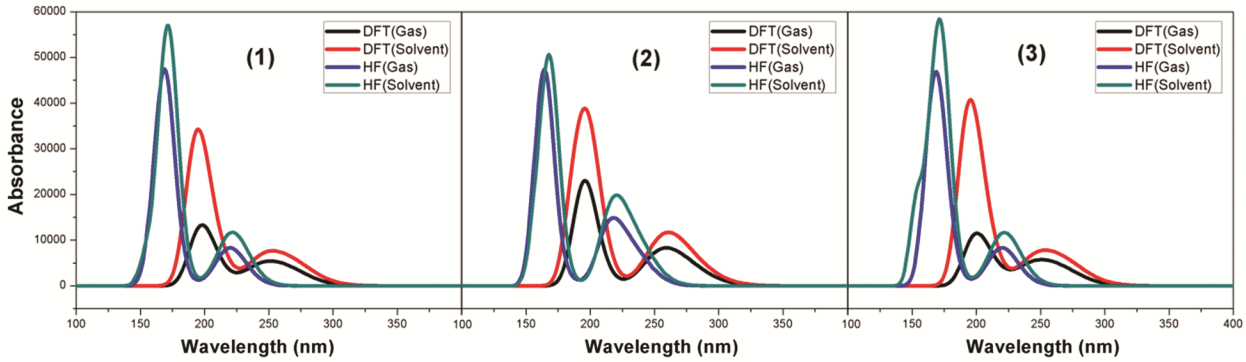

Fig. 6 — Theoretical UV spectrum of molecules (1), (2) and (3), in gas and solvent

Table 4 — Experimental and calculated absorption wavelength, oscillator strength and energy values of title molecules

Com.		B3LYP				HF			
	Transition	λ (nm)	f	E (eV)	*Major Contribution≥10%	λ (nm)	f	E (eV)	*Major Contribution≥10%
	Gases								
	I	199.72	0.018	6.207 51-56	H-3→L+1 (76%)+H-1→L+2 (11%)	170.69	0.777	7.263 54-70	HOMO→L+15 (34%), HOMO→L+16 (10%)
1	II	252.83	0.037	4.903 53-55	H-2→LUMO (97%),	216.71	0.105	5.721 53-64	H-1→L+8 (11%), H-1→L+9 (36%), H-1→L+10 (17%), HOMO→L+15 (13%)
	Ethanol								
	I	197.69	0.206	6.367 53-57	H-1→L+1 (50%), HOMO→L+6 (26%)	171.19	0.072	7.242 53-70	HOMO→L+1 (14%), HOMO→L+2 (25%), HOMO→L+4 (13%)
	II	246.28	0.132	5.034 53-55	H-1→LUMO (75%)	217.81	0.156	5.692 53-62	H-1→L+6 (13%), H-1→L+7 (43%), HOMO→L+15 (11%)
	Gases								
	I	197.11	0.036	6.2899 54-61	H-1→L+4 (15%), H-1→L+5 (28%), HOMO→L+6 (35%)	167.17	0.719	7.4165 54-71	HOMO→L+16 (36%)
	II	265.69	0.076	4.6664 54-55	HOMO→LUMO (87%)	215.92	0.329	5.7419 53-62	H-1→L+6 (19%), H-1→L+7 (54%)
2	Ethanol								
	I	199.46	0.598	6.216 54-59	H-1→L+2 (15%), HOMO→L+4 (24%), HOMO→L+5 (19%)	169.28-	1.019	7.324 54-71	HOMO→L+16 (41%), HOMO→L+17 (16%)
	II	257.73	0.231	4.810 53-55	H-1→LUMO (87%)	218.22-	0.438	5.681 53-61	H-1→L+6 (54%), H-1→L+7 (25%)
	Gas								
	I	201.48	0.058	6.153 58-64	H-2→L+1 (15%), HOMO→L+3 (67%)	171.53	0.623	7.227 58-77	H-1→L+11 (10%), HOMO→L+18 (31%), HOMO→L+19 (10%)
3	II	252.72	0.004	4.905 55-59	H-3→LUMO (96%)	223.82	0.1104	5.539 58-70	HOMO→L+11 (63%)
	Ethanol								
	I	195.52	0.184	6.341 56-61	H-2→L+1 (24%), H-2→L+2 (32%), H-2→L+3 (14%), HOMO→L+5 (10%)	173.82	0.907	7.133 58-76	H-1→L+9 (12%), HOMO→L+17 (47%)
	II	246.42	0.132	5.031 56-59	H-2→LUMO (75%), HOMO→L+2 (10%)	226.35	0.154	5.477 58-68	HOMO→L+7 (12%), HOMO→L+9 (59%)

*H=HOMO, L=LUMO

the values of the energy baariers of (2) and molecule (3) can be seen. As seen from the Fig. 7, the electron density of the HOMO is localized mostly on the benzotriazole ring except for LUMO (HF). The presence of electron-withdrawing benzotriazole at all compounds has a large effect on frontier orbitals.[21,22] The energy gap between HOMO and LUMO is a critical parameter in determining molecular electrical transport properties. This energy gap reflects the biological activity of the molecules and could be beneficial for future studies. Using the HOMO and LUMO energy values for a molecule, the following parameters can be calculated as follows:

The electronegativity (χ) is calculated using $\chi = (I + A)/2$ where I is the ionization potential, A is the electron affinity, $I = -E_{HOMO}$ and $A = -E_{LUMO}$. The chemical potential (μ) is defined as $\mu = -\chi$ and μ can be expressed as $\mu \approx (E_{HOMO} + E_{LUMO})/2$. It should be noted that, as the electronic chemical potential difference increases the global electron density transfer will have a lower polar character. As seen in Table 5, molecule (2) has a larger chemical potential than other molecules. Here, I and A are defined by the

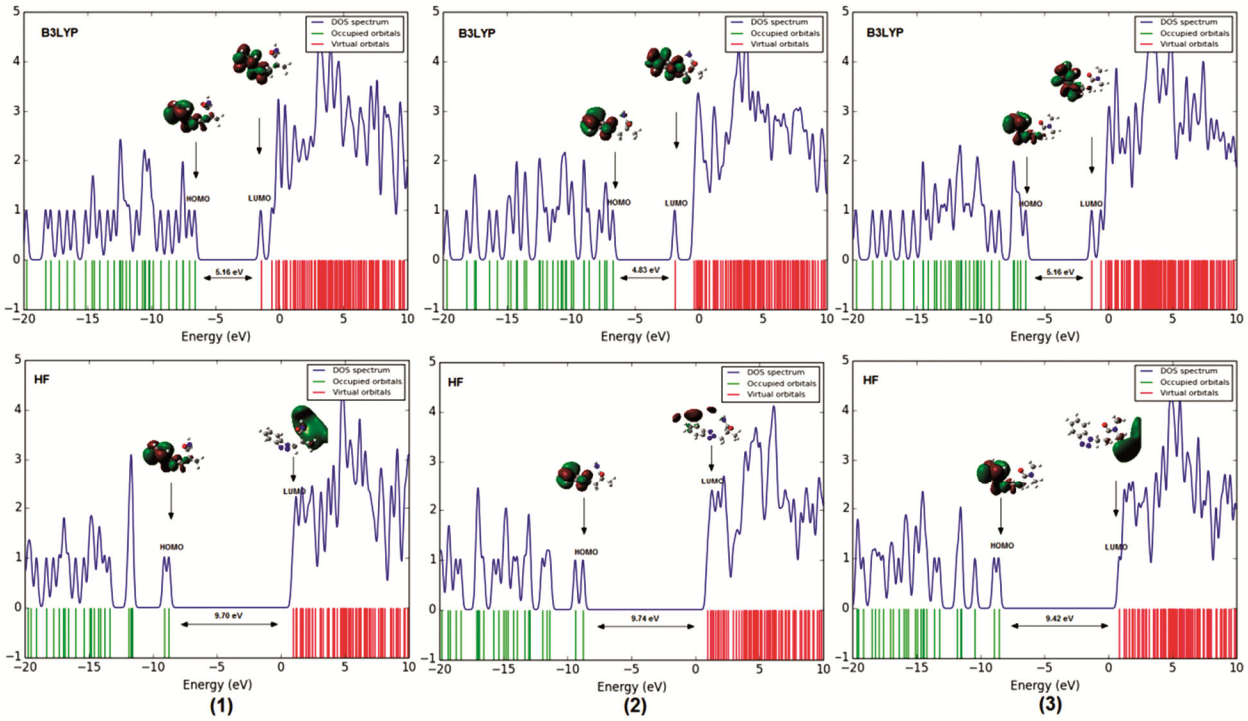

Fig. 7 — Calculated electronic total density of states (TDOS) for molecules (1), (2) and (3)

Table 5 — The measured parameters of molecules (1), (2) and (3)

Parameters (eV)	(I)		(II)		(III)	
	B3LYP	HF	B3LYP	HF	B3LYP	HF
E_{LUMO}	-1.46	0.96	-1.89	0.96	-1.31	0.85
E_{HOMO}	-6.62	-8.74	-6.72	-8.78	-6.47	-8.57
$\Delta E = E_{LUMO}-E_{HOMO}$	5.16	9.70	4.83	9.74	5.16	9.42
$A = -E_{LUMO}$	1.46	-0.96	1.89	-0.96	1.31	-0.85
$I = -E_{HOMO}$	6.62	8.74	6.72	8.78	6.47	8.57
$\chi = (I+A)/2$	4.04	3.89	4.31	3.91	3.89	3.86
$\mu = -\chi$	-4.04	-3.89	-4.31	-3.91	-3.89	-3.86
$\eta = (I-A)/2$	2.58	4.85	2.42	4.87	2.58	4.71
$S = 1/2\eta$	0.193	0.103	0.207	0.102	0.193	0.106
$w = \mu^2/2\ \eta$	3.15	1.52	3.84	1.56	2.92	1.58

frontier HOMO and LUMO energies according to the Koopman's theorem[23] and the Kohn–Sham formalism[24] within the DFT.

The resistance of a molecule to exchange electron density with the environment is defined as the chemical hardness. Chemical hardness (η) value can be calculated by the energy difference of LUMO and HOMO energies[25,26] where $\eta=(E_{LUMO} - E_{HOMO})/2$. A large HOMO–LUMO gap (ΔE_{H-L}) indicates a harder molecule and small a ΔE_{H-L} indicates a softer molecule. It is possible to relate the stability of the molecule to η, which indicates that the molecule with least ΔE_{H-L} means it is more reactive and less stable. Both of molecules (1) and (3) have larger chemical hardness which was calculated as 2.58 using B3LYP basis set and indicate hard molecules (see Table 5). Similarly chemical softness (s) is given by $S= 1/2\eta$ and the electrophilicity index, w, is defined as $w= \mu^2/2\eta$.

The quantum molecular descriptors such as electron affinity, ionization potential, electronegativity, chemical potential, chemical hardness, softness and electrophilicity index were computed similarly using the HOMO and LUMO energies, as summarized in Table 5. The calculated electrophilicity index value of molecule (2) is larger

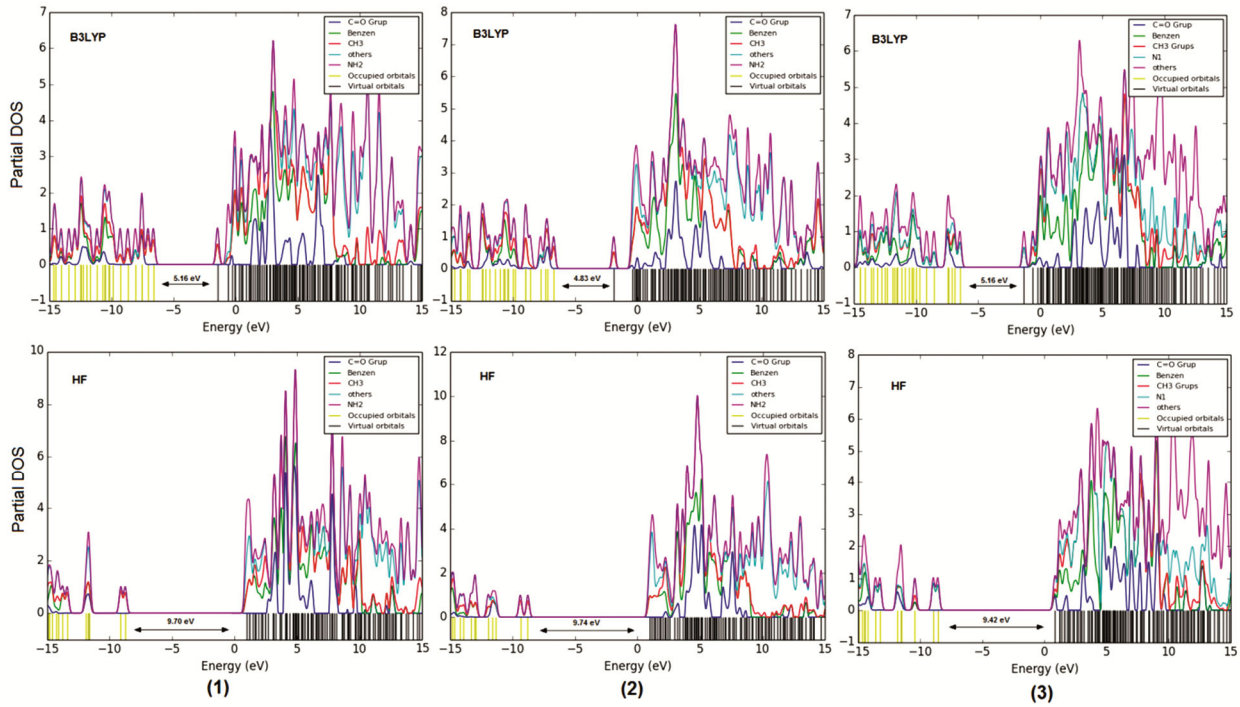

Fig. 8 — Calculated partial density of states (PDOS) for molecules (1), (2) and (3)

than the values of molecule (1) and (3). The high value of w indicates that the molecule is highly stable and dye solutions containing that molecule has higher resistance to fading when exposed to light, which is a property known as light-fastness. The measured parameters for molecules are tabulated in Table 5. Since neighbouring orbitals may show semi-degenerate energy levels in the boundary region, HOMO and LUMO energy values may not give the correct description of the frontier orbitals. In order to investigate group contributions to the HOMO and LUMO orbitals, the total density of the state (TDOS) spectrum was calculated using the Gauss-Sum 2.2 program.[27] The representation of TDOS and PDOS are given in Fig. 7 and 8. In the TDOS graphs, the green colored region shows the HOMO orbital, while the red colored region shows the LUMO orbital. The positive values of the TDOS spectrum show a bonding interaction, while the negative values indicate that there is an anti-bonding interaction (Fig. 7). The zero values of TDOS show non-bonding interactions.[28,29] The TDOS plot showed a simple view of the character of molecular orbitals in a certain energy range.

The PDOS is used to find bonding, anti-bonding and non-bonding properties according to certain fragments. The composition of fragment orbitals contributing to the molecular orbitals is represented by the PDOS spectra as shown in Fig. 8. The PDOS spectrum of all molecules can be fragmented into five groups which are assigned as C=O, benzen, CH_3, NH_2 (N for molecule 3) and others as shown in Fig. 8. For molecules(1-3), the contributions of group benzen to the PDOS of HOMO are %68 B3LYP(%77 HF), %68 B3LYP(%73 HF) and %69 B3LYP(%77 HF), respectively. Besides for (1) and (2), the contribution of group benzen to the PDOS of LUMO are %56 B3LYP(%59 HF) and %51 B3LYP(%83 HF), respectively. The contribution of group C=O and N to the PDOS of LUMO for molecule (3) are %44 and %41 in HF, while the contribution of group benzen is %55 in B3LYP. Generally, the highest contribution comes from the benzen and the least contributions from C=O. The selected group contributions can be seen in Fig. 8.

Molecular electrostatic potential (MEP)

MEP mapping is a very useful in understanding sites for electrophilic attack and nucleophilic reactions as well as hydrogen bonding interactions. Red-electron rich or partially negative charge regions of MEP were related to electrophilic reactivity and the blue-electron deficient or partially positive charge regions of MEP. In Fig. 9, the electron rich centres were found around the O atoms, and slighly N atoms (red region). Hydrogen atoms have the strongest attraction where N and O atoms have the strongest

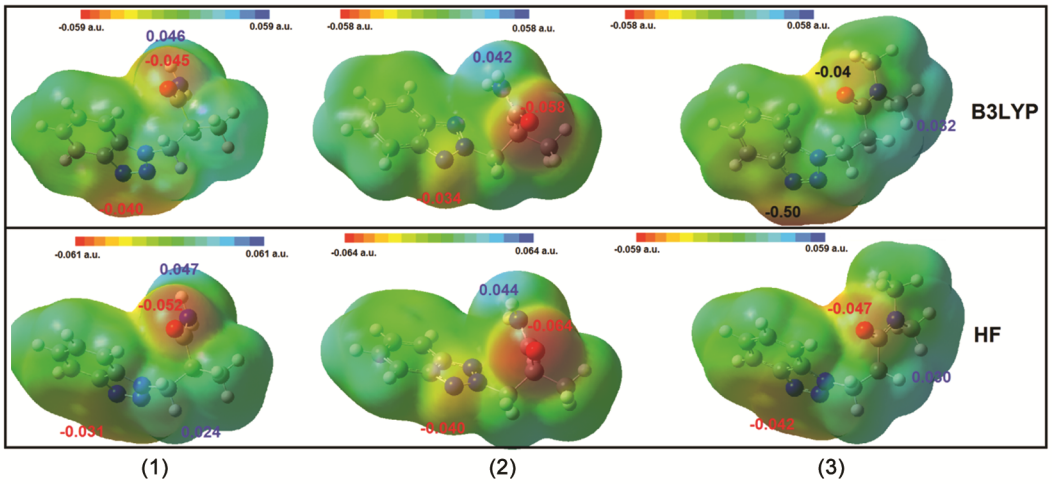

Fig. 9 — Total electron densitis mapped with the electrostatic potential surfaces

Table 6 — Thermodynamic properties at different temperatures of molecules (1), (2) and (3) calculated using B3LYP and HF.

	Molecules		*T (K)*							
			100	200	298.15	300	400	500	600	700
H (kcal mol^{-1})	(1)	B3LYP	1.579	4.678	9.281	9.383	15.718	23.500	32.471	42.396
		HF	1.546	4.487	8.783	8.877	14.775	22.068	30.553	40.019
	(2)	B3LYP	1.559	4.581	9.120	9.221	15.504	23.244	32.181	42.080
		HF	1.524	4.398	8.645	8.739	14.597	21.857	30.312	39.754
	(3)	B3LYP	1.803	5.249	10.228	10.338	17.166	25.590	35.353	46.207
		HF	1.758	5.036	9.685	9.787	16.130	24.002	33.208	43.532
	(1)	B3LYP	21.368	36.817	53.063	53.369	69.020	82.203	92.836	101.409
C (cal mol^{-1} K^{-1})		HF	20.420	34.484	49.211	49.493	64.272	77.270	88.086	96.975
	(2)	B3LYP	20.667	36.091	52.478	52.786	68.552	81.829	92.536	101.167
		HF	19.775	33.905	48.770	49.053	63.907	76.960	87.823	96.752
	(3)	B3LYP	24.792	40.370	57.321	57.647	74.666	89.388	101.467	111.319
		HF	23.842	37.886	53.114	53.412	69.345	83.773	96.008	106.194
S (cal mol^{-1} K^{-1})	(1)	B3LYP	79.707	100.574	119.082	119.424	137.540	154.851	171.176	186.460
		HF	79.382	99.205	116.487	116.804	133.667	149.889	165.327	179.902
	(2)	B3LYP	79.877	100.215	118.460	118.798	136.763	153.981	170.244	185.486
		HF	79.255	98.619	115.698	116.013	132.760	148.907	164.293	178.830
	(3)	B3LYP	85.497	108.763	128.794	129.163	148.688	167.425	185.190	201.903
		HF	84.128	106.298	125.009	125.350	143.487	160.993	177.743	193.638
G (kcal mol^{-1})	(1)	B3LYP	0.198	0.184	0.167	0.166	0.146	0.122	0.096	0.068
		HF	0.213	0.199	0.182	0.182	0.162	0.139	0.114	0.087
	(2)	B3LYP	0.199/	0.184	0.167	0.167	0.147	0.123	0.098	0.069
		HF	0.214	0.200	0.183	0.183	0.163	0.141	0.116	0.088
	(3)	B3LYP	0.224	0.209	0.190	0.190	0.168	0.143	0.114	0.084
		HF	0.242	0.226	0.208	0.208	0.187	0.162	0.135	0.106

repulsion (blue region). These sites give information about intermolecular interactions.[30]

Thermodynamic Parameters

The density functional theory is a well-established and efficient tool to predict various statistical thermodynamic properties of molecules which are important for the understanding the chemical processes. The statically thermodynamic functions: enthalpy (*H*), heat capacity (*C*), entropy (*S*) and Gibbs free energy (*G*), for the title molecule were obtained from the theoretical harmonic frequencies in the range of temperature 100-700 K and tabulated in Table 6. For an accurate prediction in determining the thermodynamic functions, we used a scale factor for frequencies (0.96).[31]

From Table 6, it can be observed that these thermodynamic functions increase as the temperature increases from 200 to 1000 K because the molecular vibrational intensities of molecules increase with temperature, along with the increase in translational and rotational energies in accordance with the equipartition theorem.[32] The correlation equations between entropies, heat capacities, enthalpy, Gibbs free energy changes and temperatures were fitted by quadratic formulas, and the corresponding fitting factors (R^2) for these thermodynamic properties are calculated for all molecules. All thermodynamic calculations were performed using the B3LYP and HF basis sets. The Gibbs free energy correlation value for all three molecules was the same for both basis sets and calculated as 0.99999. R^2 values of all molecules for S and C are close to each other while results obtained by using B3LYP calculations are slightly better than HF calculation results. But, R^2 values of enthalpy (H) of molecules (1-3) are 0.99977 (0.99986), 0.99976 (0.99985) and 0.99984 for B3LYP (HF), respectively. All of these thermodynamic data supply helpful information for further study on the molecules. The standard deviations are relatively small in the calculation of thermodynamical functions. All this thermodynamic data can be employed for further studies of the title molecule such as computing other thermodynamic energies. Here, we observed a decrease in the Gibbs free energy of the reaction, which might be useful for evaluating the spontaneity of a reaction.[33]

Nonlinear optic properties

Nonlinear optic (NLO) study is at the focus of common research because of its wide application in data storage technology, signal processing, laser technology, optical communication and optical interconnections areas. DFT has been used extensively as an effective method to investigate organic NLO materials.[34] Here we investigated non linear optical properties of all molecules using B3LYP. Here, B3LYP gives better resuls than HF according to the calculated RMSE values. Superior values of dipole moment, molecular polarizability and hyperpolarizability are required for a molecule to act as a better NLO material. Dipole moment (μ) of a molecule gives a signature about charge distribution and geometry of the molecule (Fig. 10). μ_x component of molecules 1 and 3 show the highest value for dipole moment. μ and other properties (α and β) are listed in Table 7. For example, urea is a prototypical molecule in the study of the NLO properties and

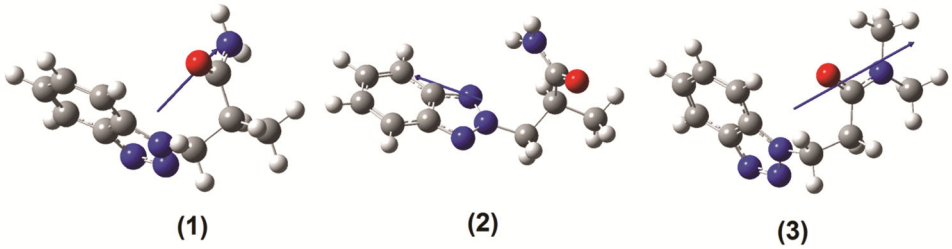

Fig. 10 — Total dipol moment of molecules (1), (2) and (3)

Table 7 — Nonlinear Optics Properties: Dipole moment (μ), polarisability (α) and hyperpolarisability (β).

	(1)	(2)	(3)		(1)	(2)	(3)
μ_x	2.14	-2.24	4.65	β_{xxx}	-53.62	-159.96	-25.30
μ_y	-1.54	0.97	1.32	β_{xxy}	10.89	18.07	-12.62
μ_z	1.03	-2.37	0.04	β_{xyy}	-5.46	4.05	31.16
μ_T	2.84	3.40	4.83	β_{yyy}	13.47	-41.72	-35.46
α_{xx}	175.93	5.03	179.86	β_{xxz}	-16.74	41.20	89.71
α_{xy}	18.35	19.78	-18.70	β_{xyz}	-13.40	-2.54	-13.02
α_{yy}	149.69	127.51	169.37	β_{yyz}	50.39	-8.62	-32.17
α_{xz}	-12.43	9.39	9.97	β_{xzz}	-22.51	-48.25	-43.86
α_{yz}	11.48	-14.61	6.83	β_{yzz}	-27.46	-25.65	-5.56
α_{zz}	115.75	122.30	130.65	β_{zzz}	-40.54	33.41	-35.57
α_T	21.77	12.57	23.67	β_T	7.081E-31	19.023E-31	5.989E-31

therefore it is frequently being used for comparative studies. The calculated values of μ, α, β for molecules 1, 2, 3 are μ = 2.84, 3.49, 4.83 Debye, α = 21.77, 12.57, 23.67 Å^3 and β = 7.08×10^{-31}, 19.0 ×10^{-31}, 5.98 ×10^{-31} cm^5/esu, which are greater than those of urea (μ = 1.3732 Debye, α = 3.8312 Å^3 and β = 3.7289 ×10^{-31} cm^5/esu) as obtained by B3LYP/6-31G(d) method.[35] A key aspect for an NLO system is the magnitude of molecular polarizability and hyperpolarizability. As a result, this molecule is a good candidate as a NLO material.

When we compare the magnitude of the β values of these molecules, we see the order of β(2) > β(1) > β(3). The larger value of hyperpolarizability corresponds to the lower HOMO–LUMO gap. This correlation is also supported with the inverse relationship as supported in Table 5, where lowest ΔE_{H-L}= 4.83 eV is seen for molecule (2). That inverse relationship was also reported previously.[36,37]

Conclusion

The calculated geometric parameters are in good agreement with the literature. Detailed vibrational assignments of the title molecule are ascribed to their structural vibrations, which show that the computed harmonic frequencies are in good agreement with their observed spectral features. According to our results on the FMO energy levels of the title molecule, we found that the corresponding electronic transfer happens between the HOMO and LUMO orbitals. Here we studied the UV-visible spectra of three different molecules (both as gas and solvent), and we found two strong bands in all three molecules using DFT (~ 200 and ~ 250 nm) and HF (~ 170 and ~ 220 nm) approximation. The MEP map indicates that hydrogen atoms are more positive in all molecules while the O atom is the most negative. These sites give information about the region from where the molecule can have intermolecular interactions and metallic bonding. This molecule is also a good candidate as an NLO material. HF and B3LYP/6-311G(d,p) calculations were further carried out to study the thermodynamic properties. The thermodynamical parameters like heat capacity, entropy and enthalpy increase as temperature is changed from 100 K to 700 K. It was found that results computed with B3LYP functional are in better agreement with experimental data as compared to the results obtained by HF.

References

1 Barot K P, Nikolova S, Ivanov I & Ghate M D, *Mini Rev Med Chem*, 13 (2013) 1421.
2 McKellar, Q A & Scott, E W, *J Vet Pharmacol Ther*, 13 (1990) 223.
3 Briguglio I, Piras S, Corona P, Gavini E, Nieddu M, Boatto G & Carta A, *Eur J Med Chem*, 97 (2015) 612.
4 Jamkhandi C M & Disouza J I, *Asian J Biochem Pharm Res*, 3 (2012) 123.
5 López-Vallejo F, Castillo R, Yépez-Mulia L & Medina-Franco J L, *J Biomol Screen*, 16 (2011) 862.
6 Borowski P, Deinert J, Schalinski S, Bretner M, Ginalski K, Kulikowski T & Shugar D, *Eur J Biochem*, 270 (2003) 1645.
7 Al-Omran F, El-Khair A A & Mohareb R M, *J Heterocycl Chem*, 39 (2002) 877.
8 Peng X M, Cai G X & Zhou C H, *Curr Top Med Chem*, 13 (2013) 1963.
9 Amenta D S, Liebing P, Biero J E, Sherman R J, Gilje J W & Edelmann F T, *Acta Crystallogr E: Crystallogr Commun*, 73 (2017) 880.
10 Frisch M J, Trucks G W, Schlegel H B, Scuseria G E, Robb M A, Cheeseman J R, Scalmani G, Barone V, Petersson G A, Nakatsuji H, Li X, Caricato M, Marenich A, Bloino J, Janesko B G, Gomperts R, Mennucci B, Hratchian H P, Ortiz J V, Izmaylov A F, Sonnenberg J L, Williams-Young D, Ding F, Lipparini F, Egidi F, Goings J, Peng B, Petrone A, Henderson T, Ranasinghe D, Zakrzewski V G, Gao J, Rega N, Zheng G, Liang W, Hada M, Ehara M, Toyota K, Fukuda R, Hasegawa J, Ishida M, Nakajima T, Honda Y, Kitao O, Nakai H, Vreven T, Throssell K, Montgomery J A, Peralta Jr J E, Ogliaro F, Bearpark M, Heyd J J, Brothers E, Kudin K N, Staroverov V N, Keith T, Kobayashi R, Normand J, Raghavachari K, Rendell A, Burant J C, Iyengar S S, Tomasi J, Cossi M, Millam J M, Klene M, Adamo C, Cammi R, Ochterski J W, Martin R L, Morokuma K, Farkas O, Foresman J B & Fox D J, *Gaussian 09, Revision A1*, (Gaussian Inc Wallingford CT) 2009.
11 Dennington R, Keith T & Millam J, *Gauss View, Version 5,* (Semichem Inc, Shawnee Mission) 2009.
12 Girma K B, Lorenz V, Blaurock S & Edelmann F T, *Z Fur Anorg Allg Chem*, 634 (2008) 267.
13 Wagner T, Hrib C G, Lorenz V, Edelmann F T, Zhang J & Yi Q, *Z Fur Anorg Allg Chem*, 638 (2012) 2185.
14 D'Amico D J, McDougal M A, Amenta D S, Gilje J W, Wang S, Hrib C G & Edelmann F T, *Polyhedron*, 88 (2015) 19.
15 Wang S, Liebing P, Oehler F, Gilje J W, Hrib C G & Edelmann F T, *Cryst Growth Des*, 17 (2017) 3402.
16 Wang S, *Synthesis and structure of supramolecular transition metal complexes containing N-benzotriazolylpropanamide and N-triazolylpropanamide,* Master Thesis, Otto von Guericke University Magdeburg, Magdeburg, Germany, 2014.
17 Eşme A, *Spectrosc Lett*, 54 (2021) 51.
18 Bhuvaneswari R, Bharathi M D, Anbalagan G, Chakkaravarthi G & Murugesan K S, *J Mol Struct*, 1173 (2018) 188.
19 Shanmugam G, Kumar K R, Sridhar B & Brahadeeswaran S, *Mater Res Bull*, 47 (2012) 2315.
20 Fleming I, *Frontier Orbitals and Organic Chemical Reactions*, (John Wiley & Sons, London) 1976.

21 Novak I & Kovač B, *J Electron Spectrosc Relat Phenom*, 113 (2000) 9.
22 Yu T, Zhao Y & Fan D, *J Mol Struct*, 791 (2006) 18.
23 Koopmans T, *Physica*, 1 (1934) 104.
24 Sham L J & Kohn W, *Phys Rev*, 145 (1966) 561.
25 Parr R G, Donnelly R A, Levy M & Palke W E, *J Chem Phys*, 68 (1978) 3801.
26 Chattaraj P K, Sarkar U & Roy D R, *Chem Rev*, 106 (2006) 2065.
27 O'boyle N M, Tenderholt A L & Langner K M, *J Comput Chem*, 29 (2008) 839.
28 Chen M, Waghmare U V, Friend C M & Kaxiras E, *J Chem Phys*, 109 (1998) 6854.
29 Abraham C S, Prasana J C, Muthu S & Raja M, *J Mol Struct*, 1160 (2018) 393.
30 Evecen M, Duru G, Tanak H & Ağar A A, *J Mol Struct*, 1118 (2016) 1.
31 Raja M, Raj Muhamed R, Muthu S & Suresh M, *J Mol Struct*, 1128 (2017) 481.
32 Ott J B & Boerio-Goates J, *Calculations from Statistical Thermodynamics,* (Academic Press, USA) 2000.
33 Murugavel S, Velan V V, Kannan D & Bakthadoss M, *J Mol Struct*, 1115 (2016) 33.
34 Tanak H, Pawlus K, Marchewka M K & Pietraszko A, *Spectrochim Acta A Mol Biomol Spectrosc*, 118 (2014) 82.
35 Sun Y X, Hao Q L, Wei W X, Yu Z X, Lu L D, Wang X & Wang Y S, *J Mol Struct: THEOCHEM*, 904 (2009) 74.
36 Delgado M C R, Hernandez V, Casado J, Navarrete J T L, Raimundo J M, Blanchard P & Roncali J, *J Mol Struct,* 651 (2003) 151.
37 Abraham J P, Sajan D, Shettigar V, Dharmaprakash S M, Němec I, Joe I H & Jayakumar V S, *J Mol Struct*, 917 (2009) 27.